

The Linear Stability of Cartesian Plumes in a Bounded Region

KHALED S. M. AL-MASHRAFI

Department of Human Resources Development, Section of Applied Sciences,
Ministry of Education, General Directorate of Education in Eastern Region South,
P.O. Box: 998, P.C. 411, Sur, Sultanate of Oman.

Khaled2014om@gmail.com

Abstract:- The flow and temperature distributions for a column of materially buoyant fluid, referred to as a Cartesian compositional plume, rising in a less buoyant fluid contained between two parallel vertical planes are identified, and the material, heat, and buoyancy fluxes associated with them are discussed. The stability of the system to linear perturbations is investigated. It is found to depend on six dimensionless numbers. The stability is discussed to find that the plume is unstable in the whole parameter space except when the plume is close to a wall and its thickness exceeds a certain value determined by the parameters of the problem, in which case a small region of stability appears in the parameter space.

Key-Words:- compositional plumes; flux; stability; growth rate; bounded domain; material diffusion

1 Introduction

Plumes are columns of fluid moving in a specific direction transporting heat and / or material. They occur in many situations in real life. Fumes emanating from chimneys of industrial establishments or from fires and polluting the surrounding environment are one form of plumes [1]. Hot material rising from the deep earth interior through the mantle and emerging on the Earth's surface as volcanoes is another form of a plume [2]. The freckles that appear in iron bars are air pockets created by a plume flow of the air trapped at the bottom when iron ore is poured down a mold or design [3].

The wide application of plume flow has generated considerable interest among researchers. A simple experiment to illustrate a real situation of plume formation is the aqueous ammonium chloride solution chilled from below [4]. The cooling from below lowers the temperature until it reaches the melting temperature of the ammonium chloride when it forms crystals releasing the lighter component (water). This process forms a layer of a mixture of solid and fluid at the bottom of the solution, which is referred to as mushy layer. As time passes and more crystals form releasing more water, the mushy layer grows in thickness and eventually becomes unstable [5] and water escapes to the top in the form of thin plumes. We shall refer to these plumes as compositional plumes since they

are a result of the difference in composition between the released water and the overlying melt of aqueous ammonium chloride. The occurrence of this phenomenon was clearly illustrated by the experiments of Copley *et al.* [6]. The need to understand the dynamics of mushy layers generated many studies (see, e.g., [7 - 27]). It is now established that mushy layers are generally unstable if they reach a certain thickness depending on the type of melt used. Ammonium chloride solution in water is the most common in experiments because it is transparent and observation and measurements are comparatively easier, although metallic and organic solutions have been studied (see, e.g., [10]).

Observations of plumes rising from mushy layers can reach the top of the melt or break up after a certain height. In an attempt to understand the dynamics of such plumes, a number of studies have been carried out. Eltayeb and Loper [28] obtained a flow structure for a fully developed plume and studied the stability of a single plume rising in an infinite fluid to find that the plume is always unstable to linear perturbations. This is found to be true whether the plume is a finite column bounded by two vertical planes or in the form of a cylinder of circular cross-section [23, 29, 30]. Further studies on the dynamics of plumes, motivated mainly by geophysical applications, have been carried out on plumes under the influence of rotation and magnetic fields [23 - 25, 31 - 35]. It is noticeable that all the theoretical studies on the dynamics of these plumes

are in unbounded domains. The present study is an attempt to investigate theoretically the influence of boundaries on the dynamics of a plume. A simple model is developed taking into account the main factors that are expected to influence the plume rising in a bounded domain. The model is illustrated in **Fig. 1**. The Cartesian geometry is used because it provides analytic solutions that allow a detailed investigation of the influence of the various parameters of the problem on its dynamics. This is expected to give results with good qualitative agreement with the more realistic form of plumes, as has been shown in [29, 30].

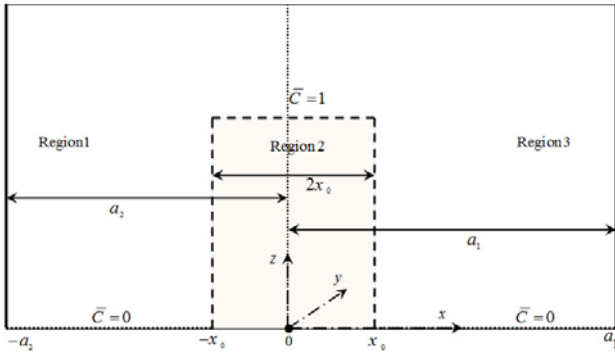


Fig. 1. The geometry of the problem showing the profile of the basic state concentration of light material representing a plume of width, $2x_0$, and concentration, 1, rising vertically in a finite fluid of width, d , and concentration, 0. Two vertical planes bound the plume on either side such that the centre of the plume is a distance a_1 from the wall on the right and a_2 from the wall on the left.

2 Formulation of the problem

We consider a two-component incompressible fluid in which the concentration of the solvent component (light material) is C and the temperature is T . The two fluids have the same kinematic viscosity, ν , and thermal diffusivity, κ . The system is governed by the equations of motion, mass, heat, concentration, and state. These equations are

$$\rho_r \left[\frac{\partial \mathbf{u}}{\partial t} + (\mathbf{u} \cdot \nabla) \mathbf{u} \right] = -\nabla p + \rho_r \nu \nabla^2 \mathbf{u} - \rho g \hat{z} \quad (1)$$

$$\nabla \cdot \mathbf{u} = 0 \quad (2)$$

$$\frac{\partial T}{\partial t} + \mathbf{u} \cdot \nabla T = \kappa \nabla^2 T \quad (3)$$

$$\frac{\partial C}{\partial t} + \mathbf{u} \cdot \nabla C = k_m \nabla^2 C \quad (4)$$

$$\frac{\rho}{\rho_r} = 1 - \alpha(T - T_r) - \beta(C - C_r) \quad (5)$$

where \mathbf{u} is the velocity vector, p the pressure, \hat{z} the uniform acceleration of gravity, \hat{z} is the upward unit vector, t the time, α the coefficient of thermal expansion, β the coefficient of compositional expansion, ρ the density, k_m is the material diffusivity, (ρ_r, T_r, C_r) reference values, and we have assumed that the fluid is Boussinesq. The equations (1) - (5) allow a hydrostatic balance governed by

$$\left. \begin{aligned} \frac{dp_h}{dz} + \rho g &= 0, & \frac{d^2 T_h}{dz^2} &= 0 \\ \mathbf{u}_h &= 0, & C_h &= C_r \end{aligned} \right\} \quad (6)$$

Motivated by the experimental work on plumes rising from mushy layers, we take a temperature profile

$$T_h = \gamma z + T_r \quad (7)$$

where γ is a positive constant so that the temperature increases with height making the fluid stably stratified thermally and any instabilities will be due to transport of material.

We now cast the equations (1) - (5) into dimensionless form. It is found that in order to maintain the effects of temperature variations and compositional variations, we use the salt-finger length scale defined by

$$L = \left(\frac{\nu \kappa}{\alpha \gamma g} \right)^{\frac{1}{4}} \quad (8)$$

and a velocity unit with the definition

$$U = \beta \tilde{C} \left(\frac{g \kappa}{\alpha \nu \gamma} \right)^{\frac{1}{2}} \quad (9)$$

so that the ensuing motions are driven by the plume flow transporting the light material, C , upwards.

Here \tilde{C} is the maximum amplitude of the concentration of light material. We further choose

$\beta \tilde{C} / \alpha$, L/U and $\rho_r \beta \tilde{C} (\nu g^3 \kappa / \alpha \gamma)^{\frac{1}{4}}$ as units of temperature, time and pressure, respectively, and express the equations in dimensionless form as

$$R \left[\frac{\partial \mathbf{u}}{\partial t} + (\mathbf{u} \cdot \nabla) \mathbf{u} \right] = -\nabla \left(p + \frac{z}{\beta \bar{C}} \right) + \left. \begin{aligned} & \nabla^2 \mathbf{u} + (T - T_r + C - C_r) \hat{z} \\ & \nabla \cdot \mathbf{u} = 0 \end{aligned} \right\}, \quad (10)$$

$$\nabla \cdot \mathbf{u} = 0, \quad (11)$$

$$R \sigma \left[\frac{\partial T}{\partial t} + \mathbf{u} \cdot \nabla T \right] = \nabla^2 T, \quad (12)$$

$$R \left[\frac{\partial C}{\partial t} + \mathbf{u} \cdot \nabla C \right] = \sigma_m \nabla^2 C. \quad (13)$$

Here the dimensionless parameters R , σ , σ_m are known as the Grashoff number, the Prandtl number and the inverse Schmidt number. They are defined by

$$R = \frac{UL}{\nu}, \quad \sigma = \frac{\nu}{\kappa}, \quad \sigma_m = \frac{k_m}{\nu}. \quad (14)$$

We define a Cartesian coordinate system $O(x, y, z)$ in which Oz is vertically upwards and Ox , Oy are horizontal with the x -axis normal to the bounding walls. The model we examine here consists of a column of fluid of finite thickness, $2x_0$, rising vertically upwards in a fluid of different concentration and bounded on either side by vertical walls, a distance d apart. We choose the origin such that the plume interfaces are situated at $x = \pm x_0$ and the walls at $x = -a_2$ and $x = a_1$ (see **Fig. 1**). The region is unbounded in the y and z directions. In comparison with the plumes observed in experiments on mushy layers (see, e.g., [16]), our model is different in that it is unbounded in the y and z directions. We feel that both assumptions can be adopted for the following reasons: First, the studies in [29, 30] showed good agreement between the stability results of the circular cylindrical plume and the Cartesian plume adopted here. Secondly, experimental work on mushy layers and the formation of plumes shows that fully developed plumes rise to heights 200 times their thickness [11], and we can approximate the situation for a fully developed plume by considering it infinite in the vertical direction.

We can now take the flow variables to have the form

$$\mathbf{u}(x, y, z, t) = \mathbf{0} + \bar{w}(x) \hat{z} + \varepsilon \mathbf{u}^\dagger(x, y, z, t), \quad (15)$$

$$C(x, y, z, t) = C_r + \bar{C}(x) + \varepsilon C^\dagger(x, y, z, t), \quad (16)$$

$$p(x, y, z, t) = p_h + \bar{p}(x) + \varepsilon p^\dagger(x, y, z, t), \quad (17)$$

$$T(x, y, z, t) = T_h + \bar{T}(x) + \varepsilon T^\dagger(x, y, z, t), \quad (18)$$

such that the variables with subscript h represent hydrostatic balance and given (in dimensionless form) by

$$T_h = T_r + \frac{(z - z_r)}{\sigma R}, \quad (19)$$

$$p_h = p_r - \frac{(z - z_r)}{\beta \bar{C}} + \frac{(z - z_r)^2}{2\sigma R}. \quad (20)$$

The variables with an ‘overbar’ are basic state variables dependent only on the horizontal coordinate x , because the horizontal variations of the vertical plume flow caused by the difference in composition between the plume and the surrounding fluid imposes a horizontal advection of temperature. The variables with a ‘dagger’ indicate a perturbation of small amplitude $\varepsilon (\ll 1)$.

Substituting the expressions (15) - (18) into the system (10) - (13), the terms independent of ε give the basic state equations, which depend on x only.

$$-\frac{d\bar{p}}{dx} \hat{x} + \left(\frac{d^2 \bar{w}}{dx^2} + \bar{C} + \bar{T} \right) \hat{z} = 0, \quad (21)$$

$$\frac{d^2 \bar{T}}{dx^2} = \bar{w}(x), \quad (22)$$

$$0 = \sigma_m \frac{d^2 \bar{C}}{dx^2}. \quad (23)$$

These equations are discussed in section 3 below.

To find the linearised perturbation equations, we subtract equations (21) - (23) from the equations (10) - (13) after substituting the variables (15) - (18). We are interested in investigating the linear stability, so we neglect the terms of order ε^2 to get the following linearised perturbation equations

$$R \left[\frac{\partial \mathbf{u}^\dagger}{\partial t} + \bar{w} \hat{z} \cdot \nabla \mathbf{u}^\dagger + (\mathbf{u}^\dagger \cdot \nabla \bar{w}) \hat{z} \right] \left. \begin{aligned} & \right\}, \quad (24) \\ & = -\nabla p^\dagger + \nabla^2 \mathbf{u}^\dagger + (T^\dagger + C^\dagger) \hat{z} \end{aligned} \right\}$$

$$\nabla \cdot \mathbf{u}^\dagger = 0, \quad (25)$$

$$\sigma R \left[\frac{\partial T^\dagger}{\partial t} + \bar{w} \frac{\partial T^\dagger}{\partial z} + \mathbf{u}^\dagger \cdot \nabla \bar{T} \right] + \mathbf{u}^\dagger \cdot \hat{z} \left. \begin{aligned} & \right\}, \quad (26) \\ & = \nabla^2 T^\dagger \end{aligned} \right\}$$

$$R \left[\frac{\partial C^\dagger}{\partial t} + \bar{w} \frac{\partial C^\dagger}{\partial z} + \mathbf{u}^\dagger \cdot \nabla \bar{C} \right] = \sigma_m \nabla^2 C^\dagger. \quad (27)$$

The perturbation equations are solved in section 4 below.

3 The Basic State

The material diffusion is taken to be negligible within the plume. In the melt, diffusion is again generally small, with σ_m taking values of the order of 10^{-3} [11]. We shall then neglect diffusion except when the plume is very close to the wall and motions between wall and plume possess small dimensions. In this situation diffusion is potent only in the boundary layer between plume and wall. It follows that for plumes away from the wall, material diffusion is negligible and the basic concentration can be chosen to possess a top-hat profile

$$\bar{C}(x) = \begin{cases} 0 & , -a_2 \leq x < -x_0 \\ 1 & , -x_0 \leq x \leq x_0 \\ 0 & , x_0 < x \leq a_1 \end{cases} \quad (28)$$

If the plume is very close to the wall, then we must use equation (23) for the narrow region between the plume and the wall. We will consider the case in which the plume is close to the wall at $x = -a_2$. The profile of the concentration is

$$\bar{C}(x) = \begin{cases} (x + a_2) / \delta & , -a_2 \leq x < -x_0 \\ 1 & , -x_0 \leq x \leq x_0 \\ 0 & , x_0 < x \leq a_1 \end{cases} \quad (29)$$

in which the thickness of the layer between sidewall and plume is

$$\delta = a_2 - x_0 (\ll 1). \quad (30)$$

Here we have imposed the condition that the concentration is continuous at the interface of the plume with the diffusive layer but its derivative is not as the matching occurs at the interface of a diffusive region with a diffusionless region.

Consider the basic state equations (21) and (22). Define

$$F(x) = \bar{T}(x) - i\bar{w}(x). \quad (31)$$

Then

$$\bar{p} = 0, \quad \frac{d^2 F}{dx^2} - iF = i\bar{C}. \quad (32)$$

The solution is subject to the boundary conditions that F and $\frac{dF}{dx}$ are continuous across the interfaces $x = \pm x_0$, and F vanishes on the sidewalls at $x = -a_2$ and $x = a_1$. If the plume is not close to a boundary, this leads to the solution

$$F = \begin{cases} F^1 & ; -a_2 \leq x < -x_0 \\ F^2 + \cosh[k(x + x_0)] - 1 & ; -x_0 \leq x \leq x_0 \\ F^3 & ; x_0 < x \leq a_1 \end{cases} \quad (33)$$

where F^1 , F^2 and F^3 are given by

$$\left. \begin{aligned} F^1 &= -A \sinh(ka_1) \sinh[k(x + a_2)] \\ F^2 &= -A \sinh(ka_1) \sinh[k(x + a_2)] \\ F^3 &= A \sinh(ka_2) \sinh[k(x - a_1)] \end{aligned} \right\} \quad (34)$$

and A and k are defined by

$$\left. \begin{aligned} A &= \frac{2 \sinh(kx_0)}{\sinh(kd)} \\ k &= \frac{1}{\sqrt{2}}(1+i), \quad d = a_1 + a_2 \end{aligned} \right\} \quad (35)$$

If the plume is close to the boundary and diffusion is potent in the narrow region between the plume and boundary, the basic state solution takes the form

$$F(x) = \begin{cases} F^4 & ; -a_2 \leq x < -x_0 \\ F^5 - 1 & ; -x_0 \leq x \leq x_0 \\ F^6 & ; x_0 < x \leq a_1 \end{cases} \quad (36)$$

where F^4 , F^5 and F^6 are given by

$$\left. \begin{aligned} F^4 &= A^{(1)} \sinh[k(x + a_2)] - \frac{x + a_2}{\delta} \\ F^5 &= A^{(1)} \sinh[k(x + a_2)] - \frac{1}{k\delta} \sinh[k(x + x_0)] \\ F^6 &= -A^{(3)} \sinh[k(x - a_1)] \end{aligned} \right\} \quad (37)$$

and $A^{(1)}$ and $A^{(3)}$ are

$$A^{(1)} = \frac{1}{\sinh(kd)} \left\{ \begin{array}{l} \cosh[k(a_1 - x_0)] \\ + \frac{\sinh[k(a_1 + x_0)]}{k\delta} \end{array} \right\}, \quad (38)$$

$$A^{(3)} = \frac{1}{\sinh(kd)} \left\{ \begin{array}{l} -\cosh[k(a_2 + x_0)] \\ + \frac{\sinh[k(a_2 - x_0)]}{k\delta} \end{array} \right\}. \quad (39)$$

A sample of the profiles of the solutions $\bar{T}(x)$ and $\bar{w}(x)$ when the plume is not very close to the boundary is plotted for different values of the plume thickness $2x_0$ in **Fig. 2**. The profiles are symmetric when the plume is situated half-way between the sidewalls. The oscillatory nature of the velocity profile introduces negative flow (i.e., downwards flow) within the plume when it is wide, and this has an effect on the net transport of material by the plume. The wide plume is also associated with a temperature profile that is almost uniform in the main body of the plume. If the position of the plume moves towards a sidewall, symmetry is broken. Here the downward flow outside the plume is partially suppressed in the narrow region between the plume and the nearest wall and strengthened on the far side. Such behaviour will lead to the modification of the modes of instability in the absence of the sidewalls.

When the solution (36) of the plume close to the boundary is compared with the solution obtained without invoking material diffusion near the boundary, we find that the two solutions are very close. A sample of the comparison is presented in **Fig. 3**. It may be concluded that the growth rate for which the basic state is important will not be affected by the material diffusion.

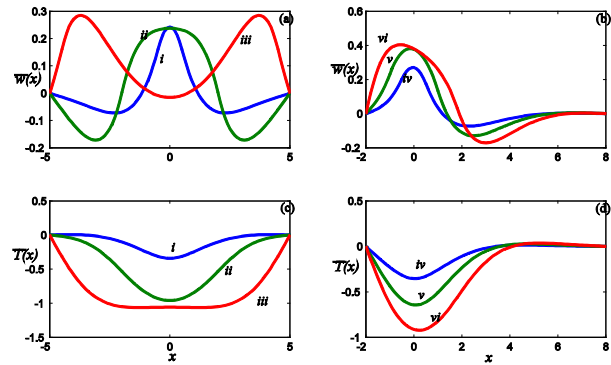


Fig. 2. The profiles of the basic state velocity, $\bar{w}(x)$, and temperature, $\bar{T}(x)$, for different values of plume thickness, $2x_0$, and distance, a_2 , from the wall on the left when $d = 10$. (a) and (c) refer to \bar{w} and \bar{T} , respectively, when the plume is positioned half-way between the two sidewalls and the labels i, ii, iii correspond to $x_0 = 0.5, 2.0, 4.5$, respectively. (b) and (d) refer to \bar{w} and \bar{T} when $a_2 = 2$ and the labels iv, v, vi correspond to $x_0 = 0.5, 1.0, 1.8$, respectively. Note that when the plume is wide, the flow is oscillatory within the plume and it slows down in the middle of the plume, while the flow of the plume is enhanced in the centre of the plume when the plume approaches the wall.

The basic state solution is associated with fluxes of heat, F_H , material, F_m , and buoyancy, F_B , which are non-dimensionalised using the units $\beta^2 \tilde{C}^2 (g \kappa^3 / \nu \alpha^7 \gamma^3)^{1/4}$, $\beta \tilde{C}^2 (g \kappa^3 / \nu \alpha^3 \gamma^3)^{1/4}$, $\beta^2 \tilde{C}^2 (g \alpha \kappa^3 / \nu \gamma^3)^{1/4}$, respectively. They are given by

$$\left. \begin{array}{l} F_H = \frac{1}{2} \int_{-a_2}^{a_1} \bar{w}(x) \bar{T}(x) dx \\ F_m = \frac{1}{2} \int_{-a_2}^{a_1} \bar{w}(x) \bar{C}(x) dx, F_B = F_H + F_m \end{array} \right\}. \quad (40)$$

The integration is straightforward and leads to

$$F_m = \frac{1}{2} \text{Im} \left\{ \frac{1}{k} \left[\begin{array}{l} 2A \sinh(kx_0) \sinh(ka_1) \sinh(ka_2) \\ -\sinh(2kx_0) \end{array} \right] \right\}, \quad (41)$$

$$F_H = \frac{-1}{4} \operatorname{Im} \left\{ \frac{1}{k} \left[\frac{\sinh^2(kx_0)}{\sinh^2(kd)} F_{H1} + A \sinh(ka_1) F_{H2} + F_{H3} \right] \right\} \quad (42)$$

where F_{H1} , F_{H2} and F_{H3} are given by

$$F_{H1} = \sinh^2(ka_1)\psi_1 - \sinh^2(ka_2)\psi_2, \quad (43)$$

$$F_{H2} = \psi_3 - \psi_4, \quad (44)$$

$$F_{H3} = \frac{\sinh(4kx_0)}{4} - 2 \sinh(2kx_0). \quad (45)$$

and we have defined

$$\psi_1 = \left\{ \sinh[2k(x_0 + a_2)] - 2k(x_0 + a_2) \right\}, \quad (46)$$

$$\psi_2 = \left\{ \sinh[2k(x_0 - a_1)] - 2k(x_0 - a_1) \right\}$$

$$\psi_3 = 2 \cosh[k(x_0 + a_2)] - \frac{1}{2} \cosh[k(3x_0 + a_2)], \quad (47)$$

$$\psi_4 = \frac{3}{2} \cosh[k(a_2 - x_0)] - 2kx_0 \sinh[k(a_2 - x_0)]. \quad (48)$$

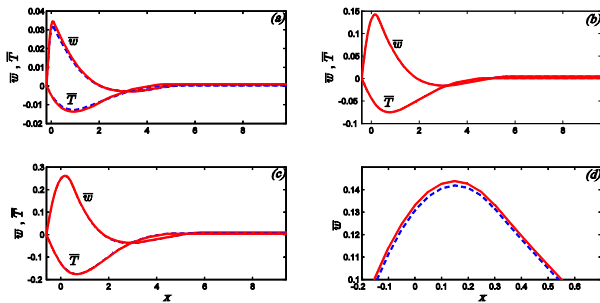


Fig. 3. Comparison of the profiles of the basic state velocity and temperature for the cases of no diffusion (broken curve) and with diffusion (solid curve) when the plume is close to a boundary , $\delta = 0.1$, $d = 10$ and x_0 takes three values (a) $x_0 = 0.1$, (b) $x_0 = 0.3$, and (c) $x_0 = 0.5$. Note that they are indistinguishable macroscopically. In (d) we show a magnified part of the curve of the case in which the difference is most pronounced (i.e., when $x_0 = 0.3$ shown in (b) and the plume is very thin) and even in this case the two profiles are very close.

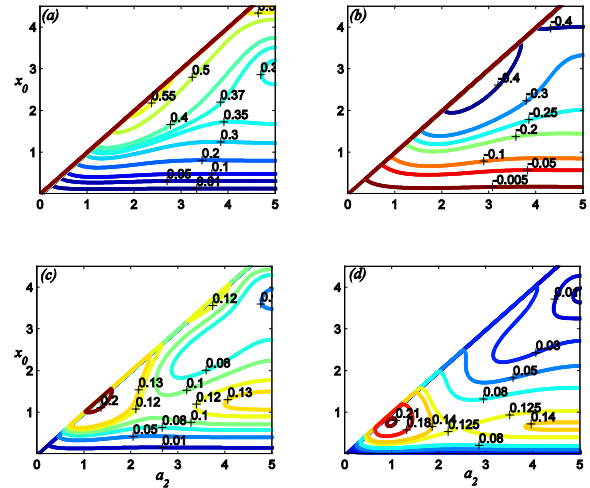


Fig. 4. The contours of the basic state fluxes of the top-hat bounded plume in the (a_2, x_0) plane ; (a) material flux, F_m , (b) heat flux , F_H , (c) buoyancy flux, F_B and (d) buoyancy flux per unit area (F_B / x_0) when $d = 10.0$. Note that the heat and material fluxes are larger at the sidewall, the buoyancy flux has a maximum value of 0.215, when $(a_2, x_0) \approx (1.22, 1.22)$ and the buoyancy flux per unit area has a maximum 0.212 at $(a_2, x_0) \approx (1, 1)$, and both maxima lie on the sidewall. The fluxes are shown for half the interval because they are symmetric about the middle plane between the sidewalls.

The fluxes are presented in the (a_2, x_0) plane in **Fig. 4**. The presence of the sidewalls has complicated the behaviour of the fluxes as compared to the case of infinite surrounding fluid. For a fixed position of the plume (i.e., fixed a_2) relative to the wall, gradual increase in the thickness of the plume is associated with an increase in the downward heat flux. For plumes of thickness less than about 2.0, the heat flux is almost a constant as the plume moves towards a sidewall. For plumes with larger thickness, the heat flux increases as the wall is approached. The upward material flux behaves similarly if the distance from the wall is less than about 4.5. For larger distances from the sidewalls, the material flux increases as x_0 increases from zero reaching a maximum before it decreases to a minimum and starts to increase again to a larger value as x_0 approaches a_2 and the plume

interface approaches a sidewall. The buoyancy flux, which is the net system flux, possesses two local maxima and a minimum. The local maximum with the largest value is situated on the boundary at $x_0 = 1.3$, while the other one is situated half-way between the two sidewalls and about the same value of x_0 . The minimum occurs for $x_0 = 3.7$ and lies half-way between the sidewalls. The buoyancy flux per unit area, illustrated in (d), has the same general behaviour as the buoyancy flux but the positions of the two local maxima and minimum are different.

4 Solution of the eigenvalue problem

In this section, we solve the eigenvalue problem posed by the perturbation equations (24) – (27) and the boundary conditions to obtain expressions for the growth rate. Our interest lies in the instability produced by the buoyant fluid in the plume. We assume that the interface at the plane $x = x_0$ is given a small harmonic disturbance of the form

$$x = x_0 + \varepsilon \exp(\Omega t + i(my - nz)) + c.c. , \quad (49)$$

where m and n are the horizontal and vertical wavenumbers, $c.c.$ refers to the complex conjugate, and Ω is a complex constant, which can be expressed as

$$\Omega = \Omega_r + i\Omega_i . \quad (50)$$

Ω_r and Ω_i will be referred to as the real and imaginary parts of Ω . The stability of the plume is determined by the sign of Ω_r . If it is negative for all possible values of the wavenumbers m and n , then the plume is stable, but the system is rendered unstable if any pair (m, n) of wavenumbers gives a positive value of Ω_r . If the preferred mode occurs for m, n both non-zero, it is referred to as a 3-dimensional mode but if any one of them vanishes it is 2-dimensional. If the maximum value of Ω_r vanishes, the plume is neutrally stable.

The disturbance (49) will propagate into the system, and affect the second interface and the variables of the system to produce the perturbations. The disturbance at the interface $x = -x_0$ can be written in the form

$$x = -x_0 + \varepsilon \eta_1 \exp(\Omega t + i(my - nz)) + c.c. \quad (51)$$

where η_1 determines the displacement of the interface at $x = -x_0$, and will be determined by the solution.

The perturbation variables produced by the disturbance (49) can be expressed in the form

$$\{u^\dagger, C^\dagger, T^\dagger, p^\dagger\} = \{-in u, nm v, w, C, T, -inp\} E \quad (52)$$

$$E = \exp(\Omega t + i(my - nz))$$

where the factors $-in$, nm , and $-in$ are introduced in the variables u , v and p , respectively, for convenience.

Substituting the variables (52) into (24) – (27), we obtain the following ordinary differential equations in x

$$Du - m^2 v + w = 0 , \quad (53)$$

$$\Delta u - Dp = R\bar{\Omega} u , \quad (54)$$

$$\Delta v - p = R\bar{\Omega} v , \quad (55)$$

$$\Delta w + T + C + n^2 p = R(\bar{\Omega} w - in u D\bar{w}) , \quad (56)$$

$$\Delta T - w = \sigma R(\bar{\Omega} T - in u D\bar{T}) . \quad (57)$$

The equation for the concentration of light material will depend on whether the plume is away from the boundary, in which case diffusion is neglected, and

$$\bar{\Omega} C = 0 , \quad (58)$$

or very close to a boundary, in which case diffusion is potent in the small region between the plume and boundary, and

$$-in \left(\frac{R}{\delta \sigma_m} \right) u = \Delta C , \quad (59)$$

in the region between plume and boundary. Here we have used

$$\left. \begin{aligned} b^2 = m^2 + n^2 , \quad D \equiv \frac{d}{dx} \\ \Delta \equiv D^2 - b^2 , \quad \bar{\Omega} = \Omega - in \bar{w}(x) \end{aligned} \right\} . \quad (60)$$

The boundary conditions across the interfaces are (see, [23, 29])

$$\left. \begin{aligned} u, v, w, T, p, C, Dv, DT \\ \text{are continuous across } x = \pm x_0 \end{aligned} \right\}, \quad (61)$$

$$\left. \begin{aligned} w'(x_0^+) - w'(x_0^-) &= \bar{C}(x_0^+) - \bar{C}(x_0^-), \\ w'(-x_0^+) - w'(-x_0^-) &= \eta_1 \{ \bar{C}(-x_0^+) - \bar{C}(-x_0^-) \} \end{aligned} \right\} \quad (62)$$

$$\left. \begin{aligned} -in u(x_0) &= \Omega - in \bar{w}(x_0) \\ -in u(-x_0) &= [\Omega - in \bar{w}(-x_0)] \eta_1 \end{aligned} \right\}. \quad (63)$$

In addition, the sidewalls are maintained at the hydrostatic temperature so that

$$u = v = w = T = C = 0 \text{ at } x = a_1, x = -a_2. \quad (64)$$

It was found that it is useful to derive the following three equations. First, differentiate (55) once and subtract (54) to get

$$\Delta \zeta = R [-in v D\bar{w} + \bar{\Omega} \zeta], \quad \zeta = Dv - u, \quad (65)$$

where ζ is related to the vertical component of vorticity. Secondly, differentiate (53) once and subtract (54) to obtain

$$n^2 u = m^2 \zeta - D(w + p) - R \bar{\Omega} u. \quad (66)$$

Thirdly, apply the operator Δ to (53) and use (54) - (56) to find

$$\Delta p - T = 2i R n u D\bar{w}. \quad (67)$$

The previous studies on a compositional plume showed that the plume flow is unstable for small value of Grashoff number [29, 30]. This dimensionless number measures the strength of the plume, resulting from the maximum amplitude of the basic concentration. It transpires that instability is also present for small values of R here too. We then write

$$\left. \begin{aligned} f(x, y, z, t) &= \sum_{r=0}^{\infty} f_r(x, y, z, t) R^r \\ \Omega &= \sum_{r=1}^{\infty} \Omega_r R^{r-1} \end{aligned} \right\}, \quad (68)$$

where $f(x, y, z, t)$ indicates any of the perturbation variables u, v, w, p, C and T .

Substituting the expressions (68) into the system (53) - (59) and the associated boundary conditions (61) - (64), and equating the coefficients of R^r ($r = 0, 1, 2, \dots$) to zero we get systems of ordinary differential equations which can be solved successively to find an expression for the growth rate. The two systems obtained for R^0 (referred to as Problem 0) and R^1 (referred to as problem 1) are sufficient to determine the stability of the interfaces, to leading order. The analysis showed that problem 0, with a growth rate $O(1)$ on the convective time scale is not affected by the basic state functions $\bar{w}(x), \bar{T}(x)$ but diffusion is important when the plume is close to a sidewall. The analysis of both cases shows that instability is present only in part of the parameter space, and it is necessary to consider the next order of the growth rate governed by Problem 1. The growth rate at $O(R)$ is strongly dependent on the basic state variables $\bar{w}(x), \bar{T}(x)$ and since the basic state is very slightly affected by diffusion (see Fig. 3), diffusion does not play an important role at this stage and the details of the analysis with diffusion is therefore not included in Problem 1. We will consider the solutions of the two problems and then discuss the results in section 5 below.

4.1 Problem 0

We will first consider the case when the plume is not too close to a sidewall and diffusion is negligible. Here equation (58) gives

$$C(x) = 0. \quad (69)$$

The coefficients of R^0 in the system (53), (55) - (57), (66) - (67) then consist of the equations

$$Du_0 - m^2 v_0 + w_0 = 0, \quad (70)$$

$$\Delta v_0 - p_0 = 0, \quad (71)$$

$$\Delta w_0 + T_0 + n^2 p_0 = 0, \quad (72)$$

$$\Delta T_0 - w_0 = 0, \quad (73)$$

$$\Delta p_0 - T_0 = 0, \quad (74)$$

$$n^2 u_0 = -D(w_0 + p_0), \quad (75)$$

noting that (65) and the appropriate conditions imply that $\zeta_0 = 0$ everywhere. Taking note of (75), the boundary conditions can then be expressed as

$$\left. \begin{aligned} (w_0 + p_0)' = v_0 = w_0 = T_0 = 0 \\ \text{at } x = a_1, x = -a_2 \end{aligned} \right\}, \quad (76)$$

$$\left. \begin{aligned} v_0, w_0, T_0, p_0, Dv_0, T_0', (w_0 + p_0)' \\ \text{are continuous across } x = \pm x_0 \end{aligned} \right\}, \quad (77)$$

$$\left. \begin{aligned} w_0'(x_0^+) - w_0'(x_0^-) = \bar{C}(x_0^+) - \bar{C}(x_0^-) \\ w_0'(-x_0^+) - w_0'(-x_0^-) = \eta_1 \{ \bar{C}(-x_0^+) - \bar{C}(-x_0^-) \} \end{aligned} \right\} \quad (78)$$

$$\left. \begin{aligned} -in u_0(x_0) = \Omega_1 - in \bar{w}(x_0) \\ -in u_0(-x_0) = [\Omega_1 - in \bar{w}(-x_0)] \eta_1 \end{aligned} \right\}. \quad (79)$$

When the plume is very close to a wall and the basic concentration given in (29) is continuous, the second condition of (78) is replaced by

$$Dw_0(-x_0^+) - Dw_0(-x_0^-) = 0. \quad (80)$$

We operate on equation (72) with Δ , and use equations (73) and (74) to get

$$\Delta^3 w_0 + \Delta w_0 + n^2 w_0 = 0. \quad (81)$$

The solution of the system (71) - (75) subject to the boundary conditions (76) - (79) is given by

$$\left. \begin{aligned} \{v_0, w_0, T_0, p_0\}^{(i)}(x) = \sum_{j=1}^3 \{1, \mu_j^3, \mu_j^2, \mu_j\} \chi_j^{(i)} \\ \chi_j^{(i)} = [A_j^{(i)} \cosh(\lambda_j x) + B_j^{(i)} \sinh(\lambda_j x)] \end{aligned} \right\}, \quad (82)$$

$$\left. \begin{aligned} u_0^{(i)}(x) = \sum_{j=1}^3 \lambda_j v_j^{(i)} \\ v_j^{(i)} = [A_j^{(i)} \sinh(\lambda_j x) + B_j^{(i)} \cosh(\lambda_j x)] \end{aligned} \right\}, \quad (83)$$

where the superscript 'i' in the solution refers to the region of the problem defined by

$$i = \begin{cases} 1 & ; -a_2 \leq x < -x_0 \\ 2 & ; -x_0 \leq x \leq x_0 \\ 3 & ; x_0 < x \leq a_1 \end{cases}, \quad (84)$$

(see **Fig. 1**) and μ_j ($j = 1, 2, 3$) are the roots of the cubic equation

$$\mu_j^3 + \mu_j + n^2 = 0, \quad (85)$$

with λ_j given by

$$\lambda_j = \sqrt{\mu_j + b^2}. \quad (86)$$

The constants $A_j^{(i)}$ and $B_j^{(i)}$ for ($i, j = 1, 2, 3$) are given by

$$\left. \begin{aligned} A_j^{(1)} = \frac{-F_j \sinh(\lambda_j a_2)}{\sinh(\lambda_j d)} [S_j^{1-} + \eta_1 S_j^{1+}] \\ S_j^{1\pm} = \sinh\{\lambda_j(x_0 \pm a_1)\} \end{aligned} \right\}, \quad (87)$$

$$\left. \begin{aligned} A_j^{(2)} = \frac{-F_j [\sinh(\lambda_j a_2) S_j^{1-} - \eta_1 \sinh(\lambda_j a_1) S_j^{2-}]}{\sinh(\lambda_j d)} \\ S_j^{2\pm} = \sinh\{\lambda_j(x_0 \pm a_2)\} \end{aligned} \right\} \quad (88)$$

$$A_j^{(3)} = \frac{F_j \sinh(\lambda_j a_1)}{\sinh(\lambda_j d)} [S_j^{2+} + \eta_1 S_j^{2-}], \quad (89)$$

$$B_j^{(1)} = \frac{-F_j \cosh(\lambda_j a_2)}{\sinh(\lambda_j d)} [S_j^{1-} + \eta_1 S_j^{1+}], \quad (90)$$

$$B_j^{(2)} = \frac{-F_j [\cosh(\lambda_j a_2) S_j^{1-} + \eta_1 \cosh(\lambda_j a_1) S_j^{2-}]}{\sinh(\lambda_j d)} \quad (91)$$

$$B_j^{(3)} = \frac{-F_j \cosh(\lambda_j a_1)}{\sinh(\lambda_j d)} [S_j^{2+} + \eta_1 S_j^{2-}], \quad (92)$$

with

$$F_j = \frac{\mu_j^2}{\lambda_j (2\mu_j + 3n^2)}. \quad (93)$$

The application of the boundary conditions (79) gives an expression for the growth rate Ω_1 and the displacement of the interface η_1 :

$$(\Omega_1/in)^2 + S_1(\Omega_1/in) + S_2 = 0, \quad (94)$$

$$\eta_1 = \frac{-N_{j-}}{(\Omega_1/in) - \bar{w}(-x_0) + M_{j+}}, \quad (95)$$

in which

$$S_1 = N_{j+} + M_{j+} - \bar{w}(x_0) - \bar{w}(-x_0), \quad (96)$$

$$S_2 = \{N_{j+} - \bar{w}(x_0)\} \{M_{j+} - \bar{w}(-x_0)\} - N_{j-} M_{j-}, \quad (97)$$

$$\left. \begin{aligned} N_{j\pm} &= \sum_{j=1}^3 \frac{-\lambda_j F_j}{\sinh(\lambda_j d)} S_j^{1-} C_j^{2\pm} \\ C_j^{2\pm} &= \cosh\{\lambda_j(x_0 \pm a_2)\} \end{aligned} \right\}, \quad (98)$$

$$\left. \begin{aligned} M_{j\pm} &= \sum_{j=1}^3 \frac{-\lambda_j F_j}{\sinh(\lambda_j d)} S_j^{2-} C_j^{1\pm} \\ C_j^{1\pm} &= \cosh\{\lambda_j(x_0 \pm a_1)\} \end{aligned} \right\}. \quad (99)$$

Thus

$$\Omega_1 = \frac{in}{2} \left(-S_1 \pm \sqrt{D_p} \right), \quad D_p = S_1^2 - 4S_2. \quad (100)$$

The properties of the roots of the cubic equation (85) render $N_{j\pm}, M_{j\pm}$ real and hence the discriminant D_p is real. It follows that Ω_1 is imaginary if $D_p \geq 0$ and complex when $D_p < 0$. In the absence of the sidewalls, the two modes are such that the two interfaces of the plume are either in phase giving a sinuous solution or out-of-phase giving a varicose solution. In both cases, Ω_1 is imaginary and the disturbances are neutral at this level of approximation of the growth rate. The introduction of the boundaries has destroyed the symmetry unless the plumes are situated halfway between the sidewalls.

It is informative to establish the relationship between the modes of the bounded plume defined by (100) and those of the unbounded one particularly that we expect the modes of the bounded plume to reduce to sinuous and varicose when the plume is positioned half-way between the two sidewalls. We take the limit $a_1, a_2 \rightarrow \infty$, and find that

$$\left. \begin{aligned} N_{j+} \rightarrow 0, N_{j-} \rightarrow \frac{1}{2} \sum_{j=1}^3 \frac{\mu_j^2 E_j}{(2\mu_j + 3n^2)} \\ \text{as } a_1, a_2 \rightarrow \infty \end{aligned} \right\}, \quad (101)$$

$$\left. \begin{aligned} M_{j+} \rightarrow 0, M_{j-} \rightarrow \frac{1}{2} \sum_{j=1}^3 \frac{\mu_j^2 E_j}{(2\mu_j + 3n^2)} \\ \text{as } a_1, a_2 \rightarrow \infty \end{aligned} \right\}, \quad (102)$$

$$\left. \begin{aligned} S_1 \rightarrow -2\bar{w}(x_0) \\ S_2 \rightarrow (\bar{w}(x_0))^2 - \left(\frac{1}{2} \sum_{j=1}^3 \frac{\mu_j^2 E_j}{(2\mu_j + 3n^2)} \right)^2 \\ \text{as } a_1, a_2 \rightarrow \infty \end{aligned} \right\}, \quad (103)$$

and

$$\left. \begin{aligned} D_p \rightarrow \left(\sum_{j=1}^3 \frac{\mu_j^2 E_j}{(2\mu_j + 3n^2)} \right)^2 \\ \text{as } a_1, a_2 \rightarrow \infty \end{aligned} \right\}, \quad (104)$$

where E_j is defined by

$$E_j = e^{-2\lambda_j x_0}. \quad (105)$$

Substituting these expressions into the equation (100) for Ω_1 , we get

$$\left. \begin{aligned} \eta_1 \rightarrow \mathfrak{m} \\ \Omega_1 \rightarrow in \left\{ \bar{w}(x_0) \pm \frac{1}{2} \sum_{j=1}^3 \frac{\mu_j^2 E_j}{(2\mu_j + 3n^2)} \right\} \\ \text{as } a_1, a_2 \rightarrow \infty \end{aligned} \right\}. \quad (106)$$

The growth rate (106) is the same as the growth rate of the Cartesian plume obtained in [29] and the values of the displacement η_1 shows that the phase of the interface at $x = -x_0$ is either out-of-phase (varicose mode) with $\eta = -1$ or in-phase (sinuous mode) with $\eta = 1$. It thus follows that the upper sign in (100) refers to a modification of the varicose mode, which we shall refer to as the modified varicose mode (MV) while the other will be denoted by the modified sinuous (MS) mode. The growth rate will be denoted by $\Omega^{(k)}$, where $k = MV, MS$ for the modified varicose and sinuous modes, respectively.

If the plume is close to the boundary then the concentration must obey the equation

$$\Delta C_0 = -in\alpha_0 u_0, \quad \alpha_0 = \frac{R}{\delta \sigma_m}, \quad (107)$$

in the thin region enclosed by the sidewall and the plume. This equation is solved subject to the conditions that the concentration must vanish on the boundary and is continuous at the interface of the plume. The equation (107) is coupled with those of p_0, w_0, T_0 through u_0 . If we eliminate all the variables in favour of w_0 , we obtain

$$(\Delta^5 + \Delta^3 + n^2 \Delta^2 - in\alpha_0 D)w_0 = 0, \quad (108)$$

and the zero order variables here are

$$\left. \begin{aligned} \{w_0, T_0, p_0\}^{(1)}(x) &= \sum_{j=1}^5 \{v_j^4, v_j^3, v_j^2\} \Phi_{cj}^{(1)} \\ \Phi_{cj}^{(1)} &= [A_j^{(1)} \cosh(\Lambda_j x) + B_j^{(1)} \sinh(\Lambda_j x)] \end{aligned} \right\} (109)$$

$$\left. \begin{aligned} \{u_0, C_0\}^{(1)}(x) &= \sum_{j=1}^5 \{v_j, -in\alpha_0\} \Lambda_j \Phi_{sj}^{(1)} \\ \Phi_{sj}^{(1)} &= [A_j^{(1)} \sinh(\Lambda_j x) + B_j^{(1)} \cosh(\Lambda_j x)] \end{aligned} \right\} (110)$$

where $\Lambda_j (j=1, 2, 3, 4, 5)$ are the roots of

$$\left. \begin{aligned} \tau_j^5 + \tau_j^3 + n\tau_j^2 - in\alpha_0 \Lambda_j &= 0 \\ \tau_j &= \Lambda_j^2 - b^2 \end{aligned} \right\}, \quad (111)$$

with a positive real part. The solutions in regions 2 and 3 are the same as those given by (82) and (83) for the diffusionless case, noting that $C = 0$ in both regions 2 and 3.

The application of the boundary conditions leads to the growth rate which has the form

$$\Omega_1 = in \{ \bar{w}(x_0) + \Omega_c(x_0, a_2, d, \alpha_0) \}, \quad (112)$$

where the expression $\Omega_c(x_0, a_2, d, \alpha_0)$ is complex and it depends on the parameters of the system. The growth rate (100) and (112) will be discussed in section 5 below.

4.1 Problem 1

The coefficients of R^1 in the perturbation equations (54) - (57), (65) - (67) give the set

$$\Delta u_1 = M_u, \quad (113)$$

$$\Delta v_1 - p_1 = M_v, \quad (114)$$

$$\Delta w_1 + T_1 + n^2 p_1 = M_w, \quad (115)$$

$$\Delta T_1 - w_1 = M_T, \quad (116)$$

$$\Delta p_1 - T_1 = M_p, \quad (117)$$

$$n^2 u_1 = m^2 \zeta_1 - D(w_1 + p_1) - \bar{\Omega}_1 u_0, \quad (118)$$

$$\Delta \zeta_1 = -im(w_0 - n^2 v_0) D \bar{w}, \quad (119)$$

in which

$$\left. \begin{aligned} M_u &= Dp_1 + (\Omega_1 - in \bar{w}) u_0 \\ M_v &= (\Omega_1 - in \bar{w}) v_0 \\ M_w &= (\Omega_1 - in \bar{w}) w_0 - in u_0 D \bar{w} \\ M_p &= 2in u_0 D \bar{w} \\ M_T &= \sigma (\Omega_1 - in \bar{w}) T_0 - in \sigma u_0 D \bar{T} \end{aligned} \right\}. \quad (120)$$

The associated boundary conditions are

$$\left. \begin{aligned} v_1 = w_1 = T_1 = D(p_1 + w_1) = 0 \\ \text{at } x = a_1, x = -a_2 \end{aligned} \right\}, \quad (121)$$

$$\left. \begin{aligned} v_1, w_1, T_1, p_1, v_1', T_1', w_1', (p_1 + w_1)' \\ \text{are continuous across } x = \pm x_0 \end{aligned} \right\}, \quad (122)$$

$$\Omega_2 = -in u_1(x_0), \quad \Omega_2 \eta_1 = -in u_1(-x_0). \quad (123)$$

The non-homogeneous system (113) - (119) can be solved in the usual form of a sum of complementary function and particular solution. Then the application of the boundary conditions (121) - (123) gives a dispersion relation for the growth rate Ω_2 . Since we are here interested mainly in obtaining an expression for the growth rate of the disturbance, we can restrict the efforts to deriving the solvability condition for the non-homogeneous system, which will lead to our requirement. The calculations lead to the growth rate Ω_2

$$\left. \begin{aligned} \Omega_2^{(k)} &= \frac{if}{n} \left[\int_{-a_2}^{a_1} \left(\Theta^{(k)} + \sum_{j=1}^3 C_j \Phi_j^{(k)} \right) dx + \hat{g}^{(k)} \right] + M_0^{(k)} \\ \Theta^{(k)} &= H^{(k)} \left(M_p^{(k)} + M_w^{(k)} \right) \\ \Phi_j^{(k)} &= H_j^{(k)} \left((\mu_j^2 + 1) M_p^{(k)} + M_w^{(k)} + \mu_j M_T^{(k)} \right) \end{aligned} \right\} (124)$$

where k takes the symbols MV or MS and $f_\eta^{(k)}$, $H^{(k)}$, $H_j^{(k)}$, C_j , $\hat{g}^{(k)}$ and $M_0^{(k)}$ are given by

$$f_\eta^{(k)} = \frac{1}{1 + (\eta_1^{(k)})^2}, \quad (125)$$

$$H^{(k)} = \left. \begin{aligned} & \left\{ \begin{array}{ll} -\hbar_1 & ; -a_2 \leq x < -x_0 \\ -\hbar_1 - \eta_1^{(k)} \hbar_3 & ; -x_0 \leq x \leq x_0 \\ \hbar_2 & ; x_0 < x \leq a_1 \end{array} \right\}, \\ & \hbar_1 = F_{1b}^{(k)} \cosh[b(x + a_2)] \\ & \hbar_2 = F_{2b}^{(k)} \cosh[b(x - a_1)] \\ & \hbar_3 = \cosh[b(x + x_0)] \end{aligned} \right\}, \quad (126)$$

$$H_j^{(k)} = \left. \begin{aligned} & \left\{ \begin{array}{ll} -\hbar_{j1} & ; -a_2 \leq x < -x_0 \\ -\hbar_{j1} - \eta_1^{(k)} \hbar_{j3} & ; -x_0 \leq x \leq x_0 \\ \hbar_{j2} & ; x_0 < x \leq a_1 \end{array} \right\}, \\ & \hbar_{j1} = F_{1j}^{(k)} \cosh[\lambda_j(x + a_2)] \\ & \hbar_{j2} = F_{2j}^{(k)} \cosh[\lambda_j(x - a_1)] \\ & \hbar_{j3} = \cosh[\lambda_j(x + x_0)] \end{aligned} \right\}, \quad (127)$$

$$C_j = \frac{-n^2}{3n^2 + 2\mu_j}, \quad (128)$$

$$\hat{g}^{(k)} = g^{(k)}(-a_2) + g^{(k)}(a_1), \quad (129)$$

$$M_0^{(k)} = in f_\eta^{(k)} \int_{-a_2}^{a_1} (\Omega_1^{(k)} - in \bar{w}) u_0^{(k)} G^{(k)} dx \quad (130)$$

and $F_{1b}^{(k)}$, $F_{2b}^{(k)}$, $F_{1j}^{(k)}$, $F_{2j}^{(k)}$, $g^{(k)}(-a_2)$, $g^{(k)}(a_1)$ and $G^{(k)}$ are defined by

$$F_{1b}^{(k)} = \frac{-1}{\sinh(bd)} \left\{ \frac{\eta_1^{(k)} \sinh(b(a_1 + x_0))}{+ \sinh(b(a_1 - x_0))} \right\}, \quad (131)$$

$$F_{2b}^{(k)} = \frac{-1}{\sinh(bd)} \left\{ \frac{\eta_1^{(k)} \sinh(b(a_2 - x_0))}{+ \sinh(b(a_2 + x_0))} \right\}, \quad (132)$$

$$F_{1j}^{(k)} = \frac{-1}{\sinh(\lambda_j d)} \left\{ \frac{\eta_1^{(k)} \sinh(\lambda_j(a_1 + x_0))}{+ \sinh(\lambda_j(a_1 - x_0))} \right\}, \quad (133)$$

$$F_{2j}^{(k)} = \frac{-1}{\sinh(\lambda_j d)} \left\{ \frac{\eta_1^{(k)} \sinh(\lambda_j(a_2 - x_0))}{+ \sinh(\lambda_j(a_2 + x_0))} \right\}, \quad (134)$$

$$g^{(k)}(a_1) = \sum_{j=1}^3 -C_j \mu_j F_{2j}^{(k)} \left(\begin{array}{l} T_1^{(k)}(a_1) \\ + \mu_j p_1^{(k)}(a_1) \end{array} \right), \quad (135)$$

$$g^{(k)}(-a_2) = \sum_{j=1}^3 -C_j \mu_j F_{1j}^{(k)} \left(\begin{array}{l} T_1^{(k)}(-a_2) \\ + \mu_j p_1^{(k)}(-a_2) \end{array} \right) \quad (136)$$

$$G^{(k)} = \frac{1}{b} \left\{ \begin{array}{ll} -\hbar_4 & ; -a_2 \leq x < -x_0 \\ (-\hbar_4 - \eta_1^{(k)} \hbar_6) & ; -x_0 \leq x \leq x_0 \\ \hbar_5 & ; x_0 < x \leq a_1 \end{array} \right\}, \quad (137)$$

$$\left. \begin{aligned} & \hbar_4 = F_{1b}^{(k)} \sinh[b(x + a_2)] \\ & \hbar_5 = F_{2b}^{(k)} \sinh[b(x - a_1)] \\ & \hbar_6 = \sinh[b(x + x_0)] \end{aligned} \right\}$$

It is noteworthy that because of the properties of the cubic equation for μ , the zeroth order variables are all real. For wavenumbers for which the zeroth order solution is neutrally stable, Ω_1 is purely imaginary and the non-homogeneity of the equations of problem 1 are all imaginary. It then follows that the variables with subscript 1 are all imaginary. When we employ this result into the expression for Ω_2 , we find that Ω_2 is real, and consequently it will determine the stability of the plume outside the unstable regions of the zeroth order.

5 Discussion

The growth rates given by the expressions(100), (112) and (124) were computed in the parameter space $(x_0, a_2, \sigma, \alpha_0, m, n)$. For a given set of the parameters $x_0, a_2, \sigma, \alpha_0$, the growth rate is maximized over m and n . The maximum value, Ω_c , of $\text{Re}(\Omega_2)$ and the corresponding wavenumbers m_c, n_c and the vertical wave speed $U_c (= \text{Im}(\Omega_c) / n_c)$ define the preferred mode of instability for that set of parameters.

First we consider equation (100). This mode is independent of σ and α_0 . As we mentioned previously, the stability of the plume at the leading order of approximation depends on D_p .

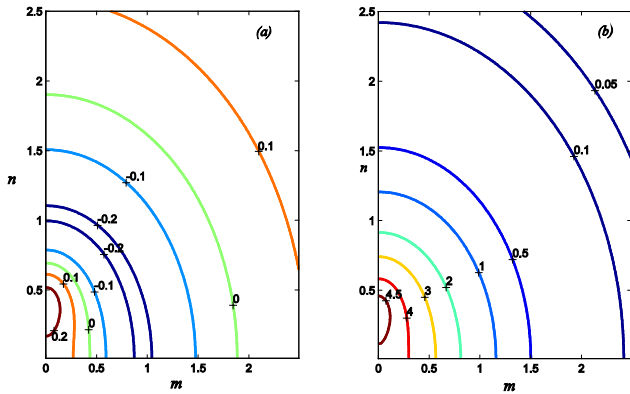


Fig. 5. The contours of the discriminant , D_p , for a plume in the absence of diffusion in the (m, n) plane when $x_0 = 0.2, d = 10.0$ for two different values of a_2 : (a) $a_2 = 0.3$ and (b) $a_2 = 2.0$. D_p here is scaled by 10^2 for ease of presentation. Note that a region of negative values of the discriminant appears in the plane when the plume is close to the wall as in (a), which indicates instability of the plume at zero order.

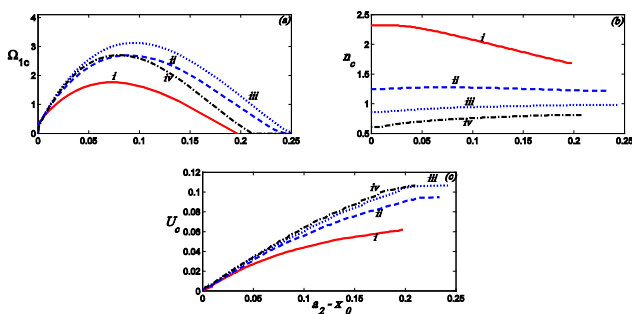


Fig. 6. The preferred mode of instability, when diffusion is negligible, with growth rate of order $O(1)$ as a function of the distance from the sidewall, $a_2 - x_0$, for four different values of x_0 ; (i) = 0.1 , (ii) = 0.2 , (iii) = 0.3 and (iv) = 0.4 , when $d = 10$. Note the dependence of the magnitude of the growth rate on the thickness of the plume and its distance from the wall.

In **Fig. 5** we show the isolines of D_p in the wavenumber plane for some representative values of x_0 and a_2 . It is found that D_p is negative for small values of x_0 and $a_2 - x_0$ indicating that instability

at zeroth order is possible only if the plume is very thin and is close to the wall. Indeed, the maximisation of the growth rate (100) when $D_p < 0$ shows that instability is possible only for values of $a_2 - x_0$ not exceeding 0.25 and the unstable modes are two-dimensional and propagate vertically upwards (**Fig. 6**). In the calculations, the discriminant and the growth rate are scaled up by 10^2 as adopted by previous authors, in order to facilitate comparison with the results in the absence of boundaries.

Next, we consider the expression when plumes are close to the wall and diffusion is important. The maximisation of the growth rate here shows that instability is again limited to short distances from the sidewall (**Fig. 7**). However, the growth rate is larger in magnitude than in the absence of diffusion and extends to a larger distance from the boundary.

Computations of the growth rate (124) showed that the plume is always unstable at a growth rate of $O(R)$. The maximum growth rate at any particular point in the parameter space (x_0, a_2, σ) can belong to the MS or the MV mode depending in a complicated way on the relative magnitudes of the parameters. As any one parameter is varied keeping the other two fixed, the preferred mode of one type can change when the parameter reaches a certain value to the other mode. Moreover, variations of a parameter can also lead to a mode of particular type (i.e., MS or MV) changing from two-dimensional to three-dimensional or the reverse when the parameter increases through a certain value. This is due to the fact that the expression (124) can possess more than one local maximum and as the parameter is increased, the larger of the two maxima decreases and the smaller increases until a value is reached when the smaller one overtakes the originally larger one and becomes preferred. **Fig. 8** illustrates such behaviour for a sample of the parameters.

In **Fig. 9** we illustrate the dependence of the preferred mode of instability on the Prandtl number, σ , in a way that allows comparison with the limiting case of no sidewalls. For small values of the Prandtl number the MS mode is preferred while the MV mode is preferred for large Prandtl numbers. This agrees well with the case of no sidewalls [30]. The value, σ_0 of the Prandtl number at which the mode changes from MS to MV depends on the distance between the plume and the nearest wall.

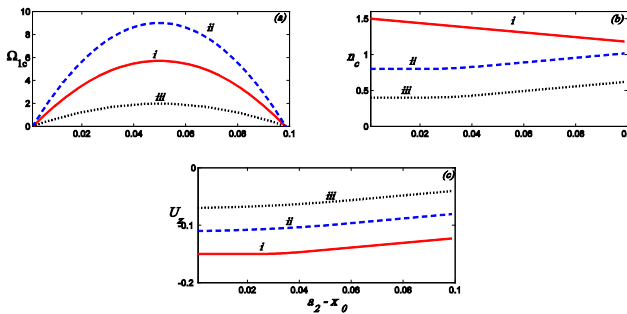


Fig. 7. The preferred mode of instability with growth rate $O(1)$ as a function of the distance from the sidewall, $a_2 - x_0$, when the plume is close to the wall and diffusion is present. Here $\alpha_0 = 1000$, $d = 10.0$ and the curves labelled i, ii, iii refer to $x_0 = 0.1, 0.3, 1.0$ respectively. Note the dependence of the magnitude of the growth rate on the thickness of the plume and its distance from a wall. In all cases, the instability is two-dimensional (with $m_c = 0$).

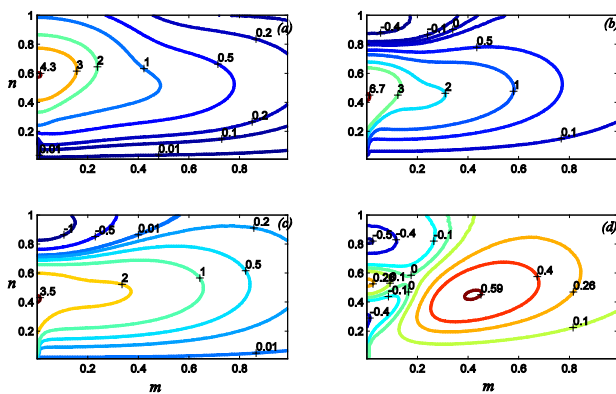


Fig. 8. Contours of the growth rate of the modes MV, as in (a) and (c), and MS, as in (b) and (d), in situations when the preferred mode changes from one type to another. Here $x_0 = 2.0$, $\sigma = 10.0$, and $d = 10$, and $a_2 = 3.0$ for (a), (b) and $a_2 = 5.0$ for (c), (d). (a), (c) refer to the MV mode and (b), (d) refer to the MS mode. Note that the MS mode is preferred for $a_2 = 3.0$ and the MV mode is preferred when $a_2 = 5.0$.

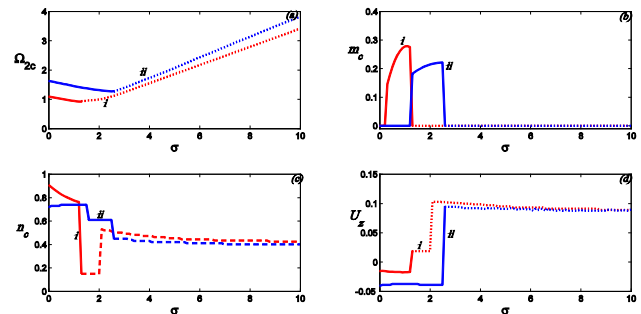


Fig. 9. Illustration of the influence of the sidewalls on the stability of the Cartesian plume. The preferred mode as a function of Prandtl number, σ , when $x_0 = 2.0$ and the plume is situated halfway between the sidewalls (i.e., $a_1 = a_2$). The curves i and ii refer to two different distances between the sidewalls: (i) $d = 10$, and (ii) $d = 20$. The solid curve refers to the MS mode while the broken one refers to the MV mode. Note the decrease in the growth rate as the distance d between the sidewalls is reduced. The presence of the boundaries also decreases the range of σ for which the MS mode is preferred.

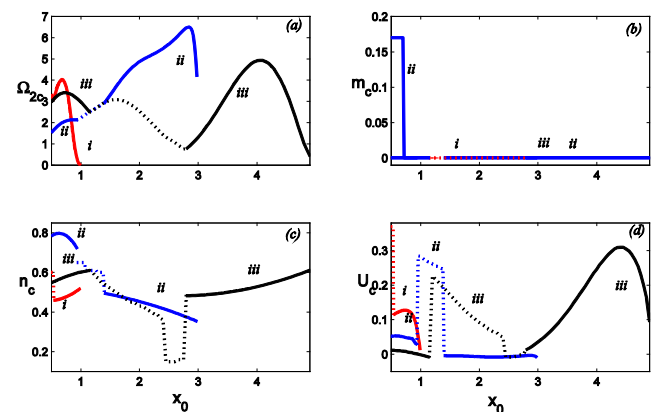


Fig. 10. The preferred mode parameters as a function of x_0 for $\sigma = 7.0$ and $d = 10.0$ for three different values of a_2 : (i) 1.0, (ii) 3.0, (iii) 5.0. The modes are two-dimensional except in the case of thin plumes when $a_2 = 3.0$. Note the complicated behaviour of the preferred mode as the thickness of the plume changes at different positions relative to the boundaries.

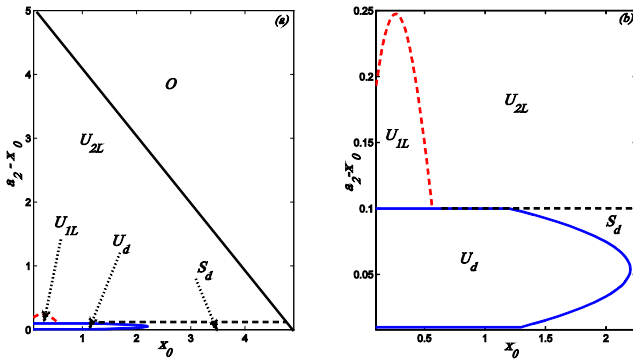


Fig. 11. The regime diagram of the bounded plume in the plane $(x_0, a_2 - x_0)$. In (a), the regions labelled U_{1L} and U_d refer to instability with growth rates of $O(1)$. U_{1L} is present when the plume is away from the walls and U_d is present when the plume is close to the wall and diffusion is important. The region marked S_d is stable and occurs when plume is close to a wall. The area labelled U_{2L} refers to instability with $O(R)$ for no diffusion. The area O is outside the domain since x_0 cannot exceeds a_2 . SubFig. (b) shows a magnification of the area for $\delta \leq 0.25$ and $x_0 \leq 2.44$ of Fig. (a). Note that the results apply to all Prandtl numbers.

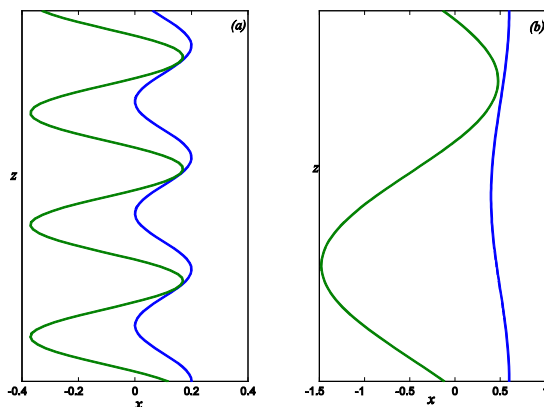


Fig. 12. A sample of the profiles of the interfaces of the unstable mode for two values of the pair (x_0, a_2) when $d = 10$. The profiles are magnified for clarity by the same factor $\varepsilon (= 0.1)$. (a) $x_0 = 0.1$, $a_2 = 0.2$, $n_c = 2.08$, $m_c = 0$ and (b) $x_0 = 0.5$, $a_2 = 0.6$, $n_c = 0.63$, $m_c = 0$. Note that the interface profiles are very close at regular intervals.

As the sidewall gets closer, σ_0 increases indicating that the presence of the boundaries tends to suppress the MV mode. The presence of the boundaries also tends to stabilise the plume as the growth rate is reduced in magnitude with the decrease in d . It is noteworthy that whatever the values of d or σ , the MS mode is three-dimensional and the MV is two-dimensional when the plume is equidistant from the sidewalls.

Fig. 10 illustrates the dependence of the preferred mode parameters on the thickness of the plume when it takes different positions relative to the sidewalls. We can observe that (i) when the plume is close to a sidewall, the preferred mode is two-dimensional (with $m_c = 0$), (ii) for moderate to large values of a_2 , the preferred mode is of the MS type when the plume is thin but changes to MV and then back to MS as it approaches the wall, (iii) in all cases the growth rate increases from its value for small thickness to a maximum before it decreases to a small value as the plume increases and approaches the sidewall.

We have now identified the growth rate at $O(1)$ and at $O(R)$ both when the plume is away from the walls, in which case diffusion is not important, and when the plume is close to a wall and diffusion is potent in the thin region between wall and plume. These results are summarised in a regime diagram in **Fig. 11**.

The preferred mode is associated with plume interfaces that are determined by (49) and (51). The amplitude at $x = x_0$ is fixed at the value 1 while the amplitude at the interface at $x = -x_0$ is determined by η_1 , which is determined by the parameters of the preferred mode for any prescribed values of x_0, a_2, σ, d . In **Fig. 12** we give samples of the profiles of the interfaces relating to some preferred modes. It is noteworthy that the interfaces are very close at regular points across the length of the plume and this may indicate a tendency to break into blobs.

5 Conclusions

The dynamics of a plume of buoyant fluid, in the form of a channel of finite width, rising in a less buoyant fluid contained between two parallel walls, a distance d apart, has been investigated. It is found that:

- (i) The plume is associated with a vertical flow that is balanced by a down flow on either side of the plume, and the flow inside the plume can develop a reverse (downward) flow around the centre of the plume if the plume is wide enough.
- (ii) The flow and concomitant temperature transport material upwards and heat downwards in such a way that the net upward buoyancy flux is positive, and possesses two local maxima and a minimum.
- (iii) Any linear disturbance of the interfaces of the plume is rendered unstable. The instability has the following main properties:
 - (a) If the plume is close to a sidewall, the instability has a growth rate $O(1)$ on the convective time scale, and is strongly affected by material diffusion provided x_0 does not exceed a certain value, otherwise the plume is stable,
 - (b) For plumes away from the sidewalls, the instability has a growth rate of $O(R)$,
 - (c) The presence of the boundaries tend to stabilise the plume when it is equidistant from the sidewalls because the growth rate of the unstable mode is reduced as the sidewalls approach the plume,
 - (d) The instability can take one of two modes, which are modifications of the sinuous and varicose modes of the plume in the absence of sidewalls but here modified by the lack of symmetry due to the different positions of the plume relative to the sidewalls,
 - (e) When the Prandtl number is small, the modified sinuous (MS) mode is preferred while the modified varicose (MV) mode is preferred for large values of the Prandtl number,
 - (f) The preferred MS mode is generally 3-dimensional while the MV mode is generally 2-dimensional,
 - (g) The profiles of the unstable plume indicate that the instability might lead to the break-up of the plume into blobs that rise to the top.
- (iv) The relatively large growth rates of the instability when the plume is close to the wall may be due to heat flux emitted by the boundary.

Acknowledgment:

The author wishes to thank the organizers of the EUROPEMENT Conferences in Saint Petersburg, Russia for their support, and the anonymous referees for their valuable comments and suggestions.

References:

- [1] McGrattan, K.B., Baum, H.R. and Rehm, R.G. Numerical simulation of smoke plumes from large oil fires, *Atmos. Environ.* 30, 1996, 4125 – 4136.
- [2] Wilson, L., Sparks, R.S.J., Huang T.C. and Watkins, N.D. The control of volcanic column heights by eruption energetics and dynamics, *J. Geophys. Res: Solid Earth* 83(B4), 1978, 1829 – 1836.
- [3] Felicelli, S.D., Heinrich, J.C., and Poirier, D.R. Simulation of freckles during vertical solidification of binary alloys, *Metallurg. Trans.* B 22 ,1991, 847 – 859.
- [4] McDonald , R.J. and Hunt, J.D. Convective fluid motions within interdendritic liquid of a casting, *Metallurg. Trans.* 1, 1970, 1787 -1788.
- [5] Worster, M.G., Instabilities of the liquid and mushy regions during solidification of alloys, *J. Fluid Mech.* 237, 1992, 649 – 669.
- [6] Copley, S.M., Giannelis, A.F., Johnson, S.M. and Hornbecker, M.F., The origin of freckles in unidirectionally solidified casting, *Metallurg. Trans.* 1 , 1970, 2193-2204.
- [7] Huppert, H.E., The fluid mechanics of solidification, *J. Fluid Mech.*, 212 ,1990, 209– 240.
- [8] Chen, C.F. and Chen, F., Experimental study of directional solidification of aqueous ammonium chloride solution, *J. Fluid Mech.*, 227, 1991, 567–586.
- [9] Tait, S., and Jaupart, C., Compositional convection in a reactive crystalline mush and melt differentiation, *J. Geophys. Res.*, 97 , 1992 , 6735–6756.
- [10] Hellawell, A., Sarazin, J.R., and Steube, R.S. Channel convection in partly solidified systems. *Phil. Trans. R. Soc. Lond.*, A345 , 1993, 507–544.
- [11] Krane, M.J.M., and Incropera, F.P., A scaling analysis of the unidirectional solidification of a binary alloy, *Int. J. Heat Mass Transfer*, 39, 1996, 3567-3579.
- [12] Worster, M.G., Convection in mushy layers, *Annual Rev. Fluid Mech.*, 29, 1997, 91 – 122.
- [13] Nishimura, T. , Wakamatsu, M., and Morega, A. M., Oscillatory double-diffusive convection in a rectangular enclosure with combined

- horizontal temperature and concentration gradients. *Int. J. Heat Mass Transfer*, 41, 1998, 1601–1611.
- [14] Jellinek, A.M., Kerr, R.C., and Griffiths, R.W., Mixing and compositional stratification produced by natural convection 1. Experiments and their application to Earth's core and mantle, *J. Geophys. Res.*, 104, 1999, 7183–7201.
- [15] Ishida, H., Yamashita, T., and Kimoto, H., Stability and chaotic characteristics of a wall plume, *Int. J. Heat Mass Transfer*, 45, 2002, 3471–3476.
- [16] Nishimura, T., Sasaki, J., and Htoo, T.T., The structure of plumes generated in the unidirectional solidification process for a binary alloy, *Int. J. Heat Mass Transfer*, 46, 2003, 4489 – 4497.
- [17] Aussillous, P., Sederman, A.J., Gladden, L.F., Huppert, H.E. and Worster, M.G., Magnetic resonance imaging of structure and convection in solidifying mushy layers, *J. Fluid Mech.*, 522, 2006, 99–125.
- [18] Guba, P., and Worster, M.G., Nonlinear oscillatory convection in mushy layers, *J. Fluid Mech.*, 553, 2006, 419 – 443.
- [19] Riahi, D.N., On the Stability of Secondary Flow in a Mushy Layer, *Proceedings of the 6th IASME/WSEAS International Conference on FLUID MECHANICS and AERODYNAMICS (FMA'08)*, Rhodes, Greece, August 20-22 2008, 93 – 98.
- [20] Okhuyseni, B.S., and Riahi, D.N., On Compositional Convection in Mushy Layers with Permeable Interface, *Proceedings of the 6th IASME/WSEAS International Conference on FLUID MECHANICS and AERODYNAMICS (FMA'08)*, Rhodes, Greece, August 20-22, 2008, 99 – 104.
- [21] Riahi, D.N., Secondary Flow in a Mushy Layer, *Proceedings of the 7th IASME/WSEAS International Conference on FLUID MECHANICS and AERODYNAMICS*, 2009, 174 – 177.
- [22] Riahi, D.N., Convection in a Horizontal Porous Layer, *Proceedings of the 7th IASME / WSEAS International Conference on HEAT TRANSFER, THERMAL ENGINEERING and ENVIRONMENT (HTE '09)*, 2009, 215 – 218.
- [23] Al-Mashrafi, K.S., and Eltayeb, I.A., The influence of boundaries on the stability of compositional plumes, *Open Journal of Fluid Dynamics*, 4, 2014a, 83 - 102.
- [24] Al-Mashrafi, K.S., and Eltayeb, I. A., The Stability of a Rotating Cartesian Plume in the Presence of Vertical Boundaries, *Open Journal of Fluid Dynamics*, 4, 2014b, 207 - 225.
- [25] Al-Mashrafi, K.S., The Mathematical Model of the Dynamics of Bounded Cartesian Plumes, *Proceedings of the 2014 International Conference on Mathematical Models and Methods in Applied Sciences (MMAS'14)*, Saint Petersburg, Russia, September 23 – 25, 2014, 345 – 357.
- [26] Pol, S. H., Fernando, J.S., and Webb, S., Evolution of double diffusive convection in low-aspect ratio containers, *Bulletin of the American Physical Society*, 55, 2010.
- [27] Dimitrova, R., Pol, S., Webb, S., and Fernando, H.J.S., Simulations of double diffusive convection in narrow containers, *J. of Engineering and Computational Mechanics*, 165, 2012, 131–145.
- [28] Eltayeb, I.A. and Loper, D.E., On the stability of vertical double-diffusive interfaces. Part1. A single plane interface, *J. Fluid Mech.*, 228, 1991, 149-181.
- [29] Eltayeb, I.A. and Loper, D.E., On the stability of vertical double-diffusive interfaces. Part 2. Two parallel interfaces, *J. Fluid Mech.*, 267, 1994, 251-271.
- [30] Eltayeb, I.A., and Loper, D.E., On the stability of vertical double-diffusive interfaces. Part 3. cylindrical interfaces, *J. Fluid Mech.*, 353, 1997, 45 - 66.
- [31] Eltayeb, I.A. and Hamza, E.A., Compositional convection in the presence of rotation, *J. Fluid Mech.*, 354, 1998, 277 – 299.
- [32] Classen, S., Heimpel, M., and Christensen, U., Blob instability in rotating compositional convection, *Geophys. Res. Lett.*, 26, 1999, 135-138.
- [33] Eltayeb, I.A., Hamza, E.A., Jervase, J.A., Krishnan, E.K., and Loper, D.E., Compositional convection in the presence of a magnetic field. II. Cartesian plume, *Proc.Roy. Soc. Lond.*, A461, 2005, 2605 – 2633.
- [34] Eltayeb, I.A., The stability of a compositional plume rotating in the presence of a magnetic fluid. *Geophys. Astrophys. Fluid Dynam.*, 100, 2006, 429-455.
- [35] Al-Lawatia, M.A., Elbashir, T.B.A., Eltayeb, I.A., Rahman, M.M., Balakrishnan, E., The dynamics of two interacting compositional plumes in the presence of a magnetic field, *Geophysical and Astrophysical Fluid Dynamics*, 105, 2011, 586 – 615.